Title: Isochronal conditions - the key to maintain the given solubility limit, of a small molecule within the polymer matrix, at elevated pressure

Author: Krzysztof Chmiel, Justyna Knapik-Kowalczuk, Marian Paluch

Citation style: Chmiel Krzysztof, Knapik-Kowalczuk Justyna, Paluch Marian. (2020). Isochronal conditions - the key to maintain the given solubility limit, of a small molecule within the polymer matrix, at elevated pressure. "Molecular Pharmaceutics" vol. 17, iss. 10 (2020), s. 3730-3739, doi 10.1021/acs.molpharmaceut.0c00463

molecular pharmaceutics

pubs.acs.org/molecularpharmaceutics

Article

Isochronal Conditions—The Key To Maintain the Given Solubility Limit, of a Small Molecule within the Polymer Matrix, at Elevated Pressure

Krzysztof Chmiel,* Justyna Knapik-Kowalczuk, and Marian Paluch

Cite This: *Mol. Pharmaceutics* 2020, 17, 3730−3739

Read Online

ACCESS | Metrics & More | Article Recommendations

ABSTRACT: In this work, we proposed the method to maintain the desired level of drug's solubility within the polymer matrix by adjusting conditions to uphold the same molecular dynamics of the system (e.g., temperature for set elevated pressure or vice versa). Namely, we observed, that recrystallization of the drug from the supersaturated drug−polymer system, initiated for the same structural relaxation time of the sample ($\tau_{\alpha\text{-}1}$) ceases when certain, different than the initial, molecular mobility of the systems is reached ($\tau_{\alpha\text{-}2}$)—regardless of a given combination of temperature and pressure conditions. Based on the presented results, one can conclude that the molecular dynamics seem to control the process of recrystallization of the excess amount of solute from the supersaturated solution (e.g., small molecules dissolved within the polymer). Therefore, it appears that the elevated pressure compensates the effect of solubility enhancement caused by the elevated temperature. Such information not only is of fundamental relevance in science but also, from a much broader perspective, could be potentially very useful considering extrusion-based manufacturing methods.

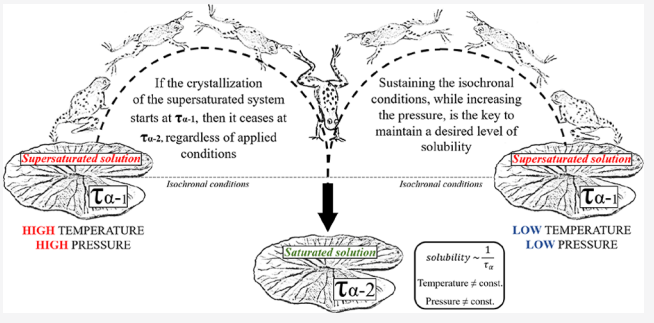

KEYWORDS: *ASD, dielectric spectroscopy, solubility, high-pressure, flutamide, Kollidon VA64*

INTRODUCTION

The solubility of small molecules (SMs) within the polymer matrixes has been of great scientific interest in the past decades.[1−6] The special case of this phenomenon considering drugs as SMs dissolved within the polymers has been extensively explored because of its importance to the pharmaceutical industry.[5,7−16] A great number of the experiments, performed under isobaric (ambient) conditions, allowed to explore the subject of drug−polymer solubility.[3,5,10,11,15,17−19] As a result of those efforts, our knowledge about this process increased. Namely, among many factors that affect the solubility of SMs within the polymer matrix, the temperature is assumed to be the most important one, governing this phenomenon.[1,20−24] Furthermore, performed studies helped to develop and improve theoretical models that allow calculating the discussed solubility. Therefore, to this day, determination of the solubility of SMs within the polymer matrix can be predicted with the use of one of the following: (i) Flory−Huggins theory;[1,20−22,25] (ii) Hansen's solubility parameter;[4,12,23] and (iii) perturbed-chain statistical associating fluid theory.[13,14,24] Nevertheless, it should be emphasized that when we compare the number of reports addressing this issue at ambient pressure conditions with those performed at elevated pressure, the significant disproportion will be found.

In a recent study, antiandrogen drug—flutamide (FL)—was dissolved within the copolymer matrix—Kollidon VA64 (PVP/VA)—and its solubility was examined at various sets of elevated temperatures and pressures.[26] On the one hand, the generally accepted dependence between temperature and solubility limit [solubility (S) is proportional to temperature: $S \sim T$] was observed regardless of applied pressure (under isobar conditions). On the other hand, the result of the increasing pressure (at constant temperature) was the reduction in the amount of FL that could be successfully dissolved within the polymer. Therefore, $S \sim T$ and at the same time, by following the cited report, solubility is inversely proportional to the applied pressure: $S \sim 1/p$. This is crucial information considering extrusion-based manufacturing methods (e.g., hot melt extrusion) because of the fact that pressures generated within an extruder can reach very high values (up to

Received: April 28, 2020
Revised: August 13, 2020
Accepted: August 13, 2020
Published: August 13, 2020

https://dx.doi.org/10.1021/acs.molpharmaceut.0c00463
Mol. Pharmaceutics 2020, 17, 3730−3739

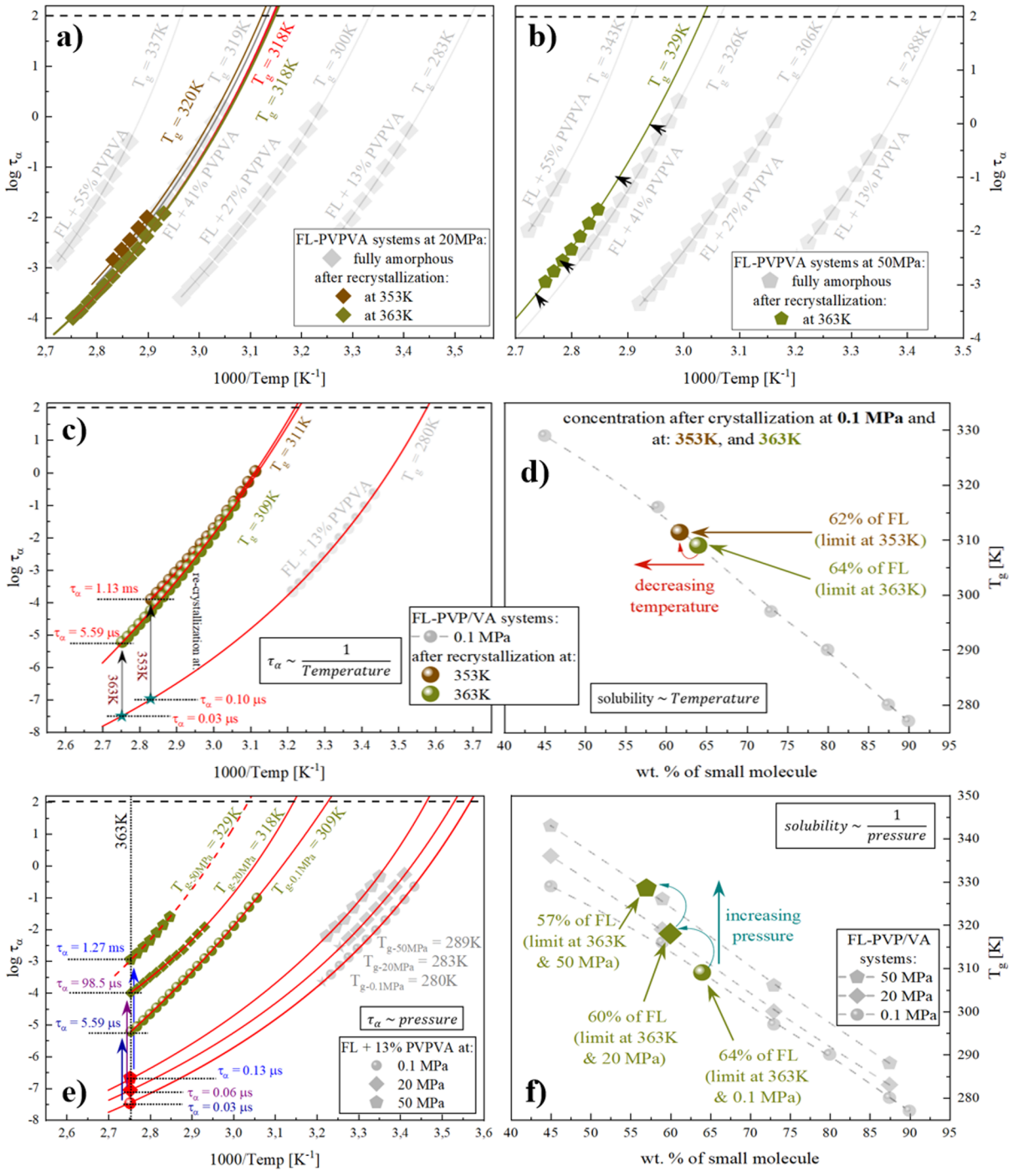

Figure 1. Data from ref 26. Upper panels present relaxation map of binary mixtures of FL with 55, 41, 27, and 13 wt % of PVP/VA at 20 MPa (a) and 50 MPa (b). Temperature dependence of τ_α in the supercooled liquid has been described by VFT equations (gray and red solid lines). Fits transferred horizontally are marked as brown and green solid lines. Left bottom and middle panels show relaxation maps of the FL + 13% PVP/VA mixture before and after the recrystallization under certain temperature and pressure conditions. (c) $\tau_\alpha(T)$ registered for the sample after isothermal crystallization at 0.1 MPA and at 343, 353, and 363 K (orange, brown, and dark green circles, respectively). (e) $\tau_\alpha(T)$ registered for the sample after isothermal crystallization at 363 K and at 0.1, 20, and 50 MPa (dark green circles, diamonds, and pentagons, respectively). $\tau_\alpha(T)$ in the supercooled liquid has been described by VFT equations (red solid lines). Red dashed line is the horizontal transfer of the VFT fit of the nearest fully amorphous concentration. Right panels present experimentally determined concentrations dependencies of the T_g of the FL-PVP/VA mixtures at 0.1 (d,f), 20 (f), and 50 MPa (f). Brown, and dark green points correspond to the concentrations obtained after the recrystallization under isothermal — 353, and 363 K, respectively — conditions. Pentagons, diamonds, and circles correspond to the concentration at certain pressure — 50, 20, and 0.1 MPa, respectively — conditions.

10,000 psi or 70 MPa),[27] especially, because it has been shown in our recent study that pressure in that range may cause the precipitation/crystallization of the original dissolved drug. By utilizing Broadband Dielectric Spectroscopy (BDS) to determine the solubility limit of the SMs (e.g., drugs) dissolved within the polymer matrixes, one can additionally monitor the

https://dx.doi.org/10.1021/acs.molpharmaceut.0c00463
Mol. Pharmaceutics 2020, 17, 3730−3739

changes occurring in the molecular dynamics of the examined system during the whole process.[8,16,26,28,29] Furthermore, the value of the structural relaxation time (τ_α) of the measured system, which reflects its molecular mobility,[30−32] can be determined during dielectric measurements. As it was proven in the case of a viscous liquid, the effect of the increasing pressure on τ_α is similar to the effect of the decreasing temperature.[33,34] Therefore, one can directly link it to temperature (as inversely proportional to) and pressure (as proportional to) in the following fashion: $\tau_\alpha \sim 1/T$ and $\tau_\alpha \sim p$.[35−38]

The central idea behind the present work is to provide an easy and simple way to determine the conditions needed to maintain a given level of the solubility under various pressures (temperature adjustment to prevailing pressure conditions). This is based on two parameters τ_α and S. Given their inverse dependence on temperature and pressure: $S \sim T/p$ and $\tau_\alpha \sim p/T$,[33−38] their mutual relation can be considered. If that is the case, then solubility should be inversely proportional to the τ_α of the system ($S \sim 1/\tau_\alpha$) at the beginning of crystallization. This would mean that, regardless of the chosen temperature or pressure, while maintaining the isochronal conditions, one should always obtain the same limiting concentration. In order to facilitate the investigation, we decided to perform the necessary analysis on the system well-characterized under both ambient and elevated pressure conditions—FL-PVP/VA.[16,26] Furthermore, in order to determine the solubility limit of the system under compression as well as to determine its τ_α, we utilized BDS.

EXPERIMENTAL SECTION

Materials. FL drug of molecular mass MW = 276.21 g mol^{-1} and purity ≥99% was purchased from Sigma-Aldrich and used without further purification. Poly vinylpyrrolidone vinylacetate — Kollidon VA64 (PVP/VA) of molecular mass MW = 45,000−47,000 g mol^{-1} was purchased from BASF SE (Ludwigshafen, Germany). The sample was received as a white powder and used without further purification.

The glass-transition temperature of the bulk polymer determined from the differential scanning calorimetry (DSC) measurements is 376 K (recorded on a second heating run, after cooling from 420 to 265 K with a cooling rate of 20 K/min). From the dielectric relaxation studies, we get T_g = 376 K (defined as a temperature at which τ_α = 100 s, data not shown).

The glass-transition temperature of the drug determined from the DSC measurements is 274 K (recorded on a second heating run, after cooling from 410 to 253 K with a cooling rate of 20 K/min). From the dielectric relaxation studies, we get T_g = 271 K (defined as a temperature at which τ_α = 100 s).[16]

Preparation of Binary Systems. To acquire homogeneous samples, we mixed the compound with the polymer at appropriate ratios in a mortar. Sample preparation for the BDS and high-pressure BDS measurements involved melting at T = 410 K, followed by vitrification on a previously chilled copper plate. All measurements were performed immediately after the preparation of the amorphous systems to avoid recrystallization.

Broadband Dielectric Spectroscopy. The dielectric measurements of FL-based ASDs were carried out using a Novo-Control GMBH Alpha dielectric spectrometer (Montabaur, Germany) in the frequency range from 10^{-1} to 10^6 Hz at given temperatures with a heating rate ∼ 0.5 K/min. The temperature was controlled by a Quatro temperature controller with temperature stability better than 0.1 K. Dielectric studies of FL and its binary systems were performed immediately after its vitrification by fast cooling of the melt in a parallel-plate cell made of stainless steel (diameter 15 mm and a 0.1 mm gap with quartz spacers).

For the high-pressure BDS measurements, we additionally employed a high-pressure Unipress U111 setup (Warszawa, Poland). Herein, the sample was measured in a similar, made of stainless steel, parallel-plate cell (diameter of 15 mm and a 0.1 mm gap with Teflon spacers). It was sealed and mounted by a Teflon tape to separate it from the silicon liquid. The temperature was adjusted with a precision of 0.1 K by the Julabo heating circulator (Seelbach, Germany).

RESULTS AND DISCUSSION

In order to test the validity of the proposed idea, we performed the series of dielectric measurements under various temperature and pressure conditions and additionally analyzed recently published data of FL-PVP/VA.[26] The initial part of this study will focus on the analysis of the already published data, especially on the temperature dependencies of the relaxation times of the FL-PVP/VA systems under various pressure conditions. The detailed analysis of obtaining such dependency is described along the experimental part later on. In recalled paper, we determined the solubility limit of FL within the polymer matrix under both ambient and elevated pressure conditions. Figure 1 shows the temperature dependence of the α-relaxation time [$\tau_\alpha(T)$] registered for the FL + 13 wt % of PVP/VA sample both before (gray circles) and after isothermal crystallization at 0.1, 20, and 50 MPa and at 353 and 363 K (brown and green symbols, respectively). Temperature evolution of the structural relaxation time — in supercooled liquid region — usually shows non-Arrhenius-like behavior. Hence, in order to parameterize it, we used the Vogel−Fulcher−Tamman (VFT) equation that is defined as follows[39−41]

$$\tau_\alpha(T) = \tau_\infty \exp\left(\frac{B}{T - T_0}\right) \quad (1)$$

where τ_∞, B, and T_0 are the fitting parameters. It has to be pointed out that in the case of some of the measurements, performed at elevated pressure (e.g., FL + 13 wt % of PVP/VA system after recrystallization at at 363 K and 20 MPa), the number of the experimentally determined τ_α after recrystallization is not sufficient to parameterize it well with the VFT equation (see brown diamond in Figure 1a). However, because of the close proximity of different, well-parameterized concentrations: FL + 41 wt % of PVP/VA (VFT fit presented as dark gray solid line in Figure 1a,b), we decided to transfer horizontally its VFT fit to match determined $\tau_\alpha(T)$. Validation of the proposed approach can be seen in case of the recrystallization of the FL + 13 wt % of PVP/VA at 363 K and 20 MPa — Figure 1a — the horizontally transferred fit of the fully amorphous FL + 41 wt % of PVP/VA system registered at 20 MPa (green line) is in very good agreement with the VFT fit of the experimental points of the system registered after recrystallization at 363 K and 20 MPa (red solid line). Glass-transition temperature determined in both cases is equal to 318 K.

https://dx.doi.org/10.1021/acs.molpharmaceut.0c00463
Mol. Pharmaceutics 2020, 17, 3730−3739

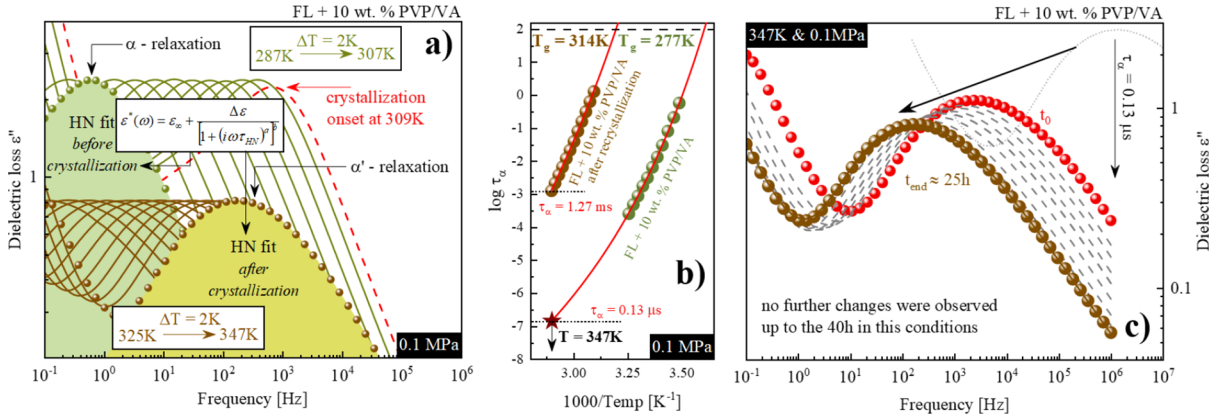

Figure 2. Data presented in this figure were obtained at ambient pressure conditions . (a) Dielectric spectra obtained for the fully amorphous sample as well as the sample during additional measurements performed after crystallization at 347 K, green and brown solid lines, respectively. Green and yellow shaded areas correspond to the fit acquired by the Havriliak–Negami (HN) function to the spectrum of fully amorphous and partially recrystallized sample presented as the green and brown circles, respectively. (b) $\tau_\alpha(T)$ registered for the fully amorphous as well as the FL + 10 wt % PVP/VA sample after isothermal crystallization at 347 K. Temperature dependence of τ_α in the supercooled liquid state has been described by VFT equations (red solid lines). (c) Dielectric spectra obtained during the isothermal crystallizations registered at 347 K. t_0 indicates the first recorded spectrum at the set temperature, and it does not correspond to the beginning of the crystallization. The light gray dotted spectrum was not obtained during any measurement — it is presented to help visualize set relaxation time.

From the extrapolation of the VFT fit up to the temperatures of the isothermal crystallization, we were able to determine the initial τ_α of the system (see Figure 1c,e). It has to be pointed out that its experimental determination would be impossible because of the sample's vast tendency toward recrystallization.[26] As can be seen, the relaxation time of the system becomes shorter as the temperature increases, which is a well-known phenomenon. However, focusing on the solubility limits determined in ref 26, one can observe that besides the fact that with increasing temperature (at constant pressure) the solubility of FL in the polymer matrix increases (which is consistent with data reported in the case of different pharmaceuticals[5,10,11,15,17−19,42,43]), the conditions that correspond to the longest relaxation time at the beginning of the recrystallization result in the lowest amount of the drug that can be successfully dissolved within the polymer (see Figure 1d). This would also not be a surprising phenomenon considering mutual dependence between the temperature and relaxation time observed in Figure 1c.

At this point, it should be mentioned that τ_α does not depend solely on the temperature but can be affected by the pressure as well.[33,34] Therefore, we performed additional analysis on the recalled results obtained under elevated pressure conditions (see Figure 1e). As can be seen, the relaxation time is getting longer as the pressure elevates, which is an effect similar to the lowering of the temperature and has already been observed.[33,34] Accordingly, the highest amount of the FL, which can be effectively dissolved within the Kollidon VA64 matrix, is related to the conditions that correspond with the shortest relaxation time. Based on these examples, we propose the idea that the mentioned solubility is inversely proportional to the relaxation time of the system.

Throughout aforementioned steps we confirmed the following facts about the FL-PVP/VA systems: (i) τ_α of this system is proportional to the pressure and inversely proportional to the temperature ($\tau_\alpha \sim p/T$); (ii) solubility of the FL within the PVP/VA matrix is proportional to the temperature and inversely proportional to the pressure ($S \sim T/p$).

Considering proposed idea, one should obtain the same limiting concentration while maintaining the same molecular dynamics of the system, regardless of the chosen temperature or pressure. Therefore, in the following part of this study, we focus on the conducted measurements. We performed crystallization studies at which the sample was stored under isochronal conditions (at various sets of temperature and pressure conditions that were chosen with regard to the fully amorphous sample). We have chosen τ_α = 0.13 μs, τ_α = 0.52 μs, and τ_α = 2.7 μs for our measurements because of the fact that the recrystallization under these conditions should progress relatively fast.

The representative dielectric loss spectra of the FL+ 10 wt % PVP/VA mixture which were obtained during heating, above sample's glass-transition temperature (T_g), are shown in Figure 2a. The presented spectra exhibit one well-resolved loss peak corresponding to the structural—α—relaxation. The intensity of this peak slightly decreases as it moves toward higher frequencies with the increasing temperature up to 307 K. Above this temperature (i.e., at 309 K), one can observe a substantial decrease of the dielectric strength ($\Delta\varepsilon$), which corresponds to the considerable drop in the intensity of the structural relaxation peak. By acknowledging the fact that $\Delta\varepsilon$ is proportional to the number of units involved in structural relaxation, the discussed rapid drop would indicate the onset of the sample's recrystallization.[44,45]

To obtain the values of τ_α at various temperatures and consequently determine the temperature dependencies of the α-relaxation times for all examined systems, dielectric spectra collected above the sample's glass-transition temperature (T_g) were fitted using the HN function[46]

$$\varepsilon^*(\omega) = \varepsilon_\infty + \frac{\Delta\varepsilon}{[1 + (i\omega\tau_{HN})^a]^b} + \frac{\sigma_{dc}}{\varepsilon_0 i\omega} \quad (2)$$

where ε_∞ is high-frequency limit permittivity, ε_0 is the permittivity of vacuum, $\Delta\varepsilon$ is dielectric strength, ω is equal to 2πf, τ_{HN} is the HN relaxation time, a and b are the parameters that represent symmetric and asymmetric broadening of relaxation peak, σ_{dc} is the dc conductivity, and ε_0 is the dielectric permittivity of the vacuum (the example of the HN fitting is presented in Figure 2a as the shaded area). Using the

https://dx.doi.org/10.1021/acs.molpharmaceut.0c00463
Mol. Pharmaceutics 2020, 17, 3730−3739

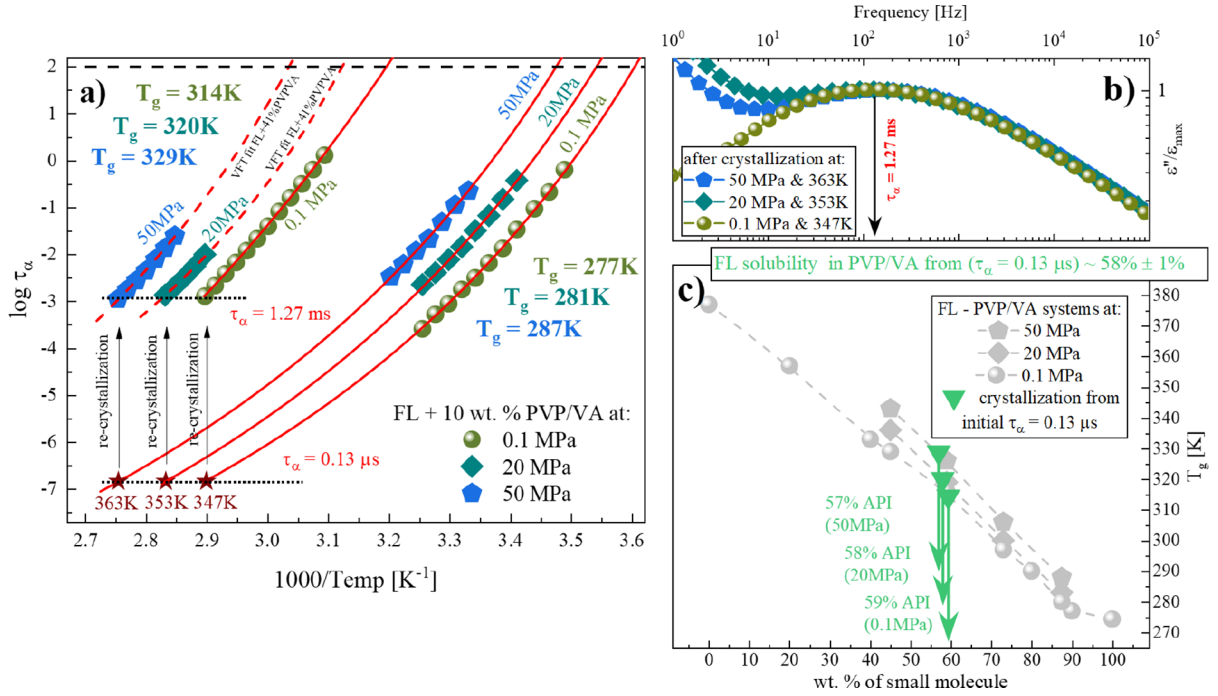

Figure 3. (a) $\tau_\alpha(T)$ registered for the fully amorphous FL + 10 wt % PVP/VA sample (blue pentagons, green diamonds, and dark green circles for 50, 20, and 0.1 MPa, respectively) as well as the sample after isothermal crystallization at (i) 363 K and 50 MPa; (ii) 353 K and 20 MPa; and (iii) 347 K and 0.1 MPa (blue pentagons, turquoise diamonds, and dark green circles, respectively). $\tau_\alpha(T)$ in the supercooled liquid has been described by VFT equations (red solid lines). Red dashed line is the horizontal transfer of the VFT fit of the nearest fully amorphous concentration (see Figure 1a,b). (b) Dielectric spectra obtained after the isothermal and isobar crystallization under given conditions. (c) Experimentally determined concentrations dependencies of the T_g of the FL-PVP/VA mixtures at 0.1, 20, and 50 MPa (gray circles, diamonds, and pentagons, respectively). Light green triangles correspond to the concentrations obtained after the recrystallization under isochronal — τ_α = 0.13 μs — conditions.

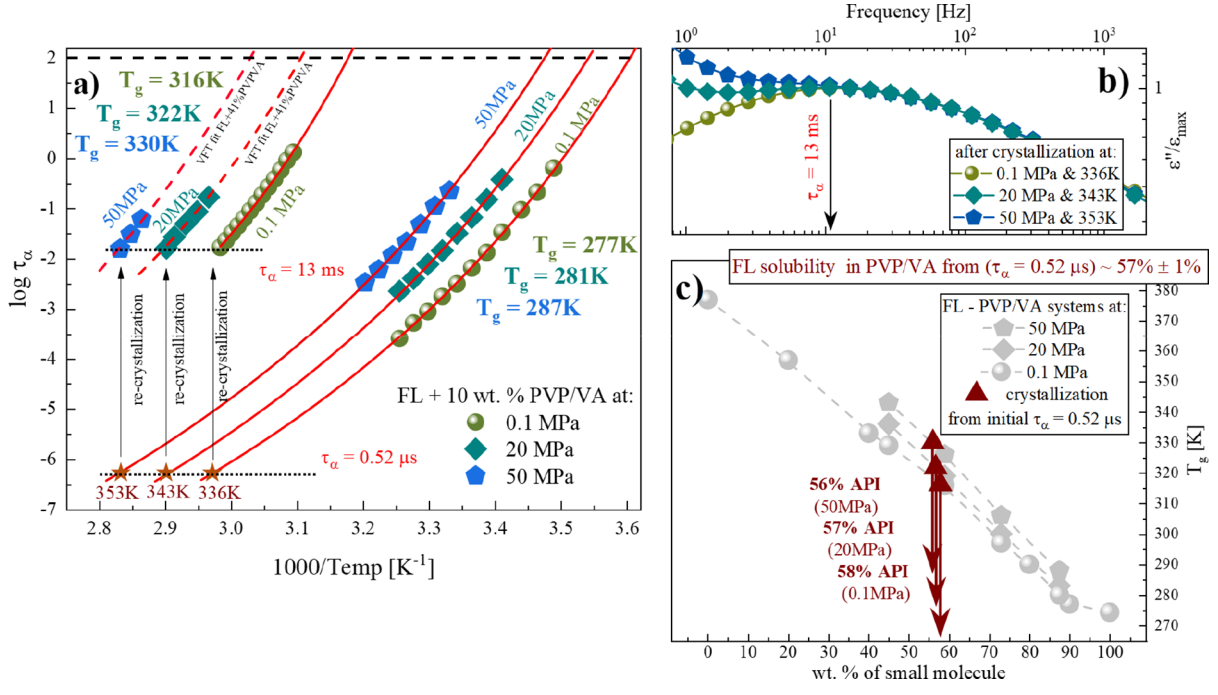

Figure 4. (a) $\tau_\alpha(T)$ registered for the fully amorphous FL + 10 wt % PVP/VA sample (blue pentagons, green diamonds, and dark green circles for 50, 20, and 0.1 MPa, respectively) as well as the sample after isothermal crystallization at (i) 353 K and 50 MPa; (ii) 343 K and 20 MPa; and (iii) 336 K and 0.1 MPa (blue pentagons, turquoise diamonds, and dark green circles, respectively). $\tau_\alpha(T)$ in the supercooled liquid has been described by VFT equations (red solid lines). Red dashed line is the horizontal transfer of the VFT fit of the nearest fully amorphous concentration (see Figure 1a,b). (b) Dielectric spectra obtained after the isothermal and isobar crystallization under given conditions. (c) Experimentally determined concentrations dependencies of the T_g of the FL-PVP/VA mixtures at 0.1, 20, and 50 MPa (gray circles, diamonds, and pentagons, respectively). Wine triangles correspond to the concentrations obtained after the recrystallization under isochronal — τ_α = 0.52 μs — conditions.

https://dx.doi.org/10.1021/acs.molpharmaceut.0c00463
Mol. Pharmaceutics 2020, 17, 3730−3739

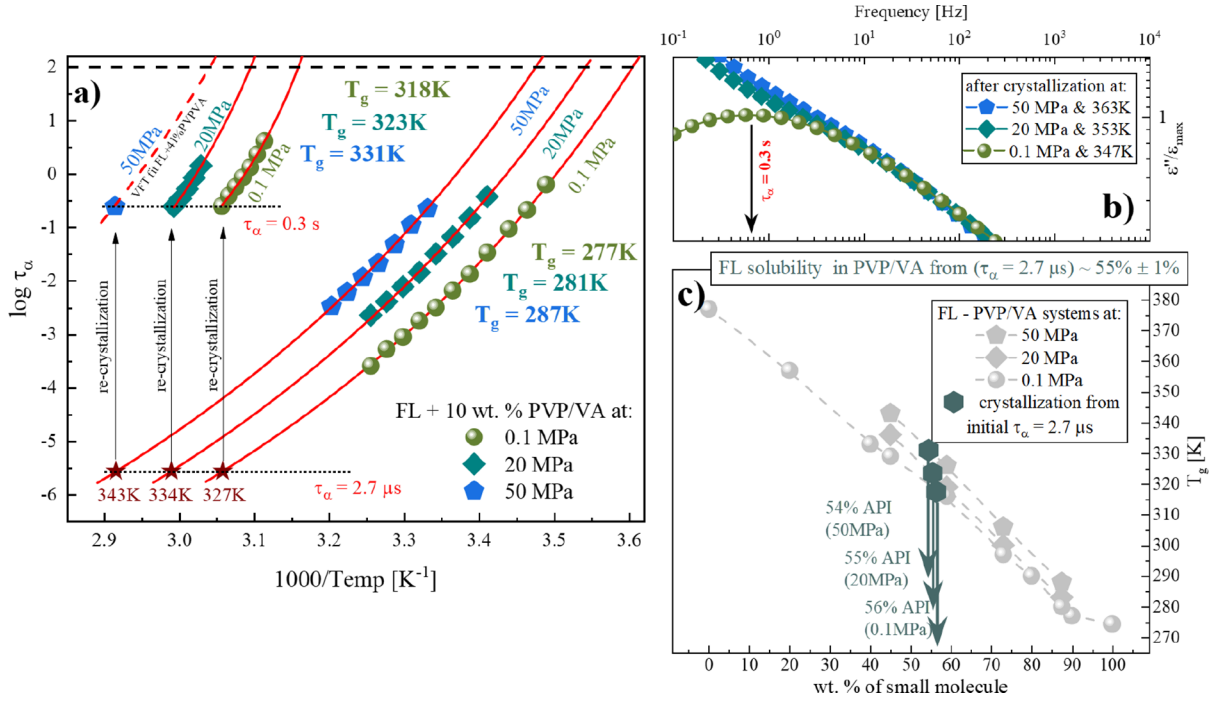

Figure 5. (a) $\tau_\alpha(T)$ registered for the fully amorphous FL + 10 wt % PVP/VA sample (blue pentagons, green diamonds, and dark green circles for 50, 20, and 0.1 MPa, respectively) as well as this sample after isothermal crystallization at (i) 343 K and 50 MPa; (ii) 334 K and 20 MPa; and (iii) 327 K and 0.1 MPa (blue pentagons, turquoise diamonds, and dark green circles, respectively). $\tau_\alpha(T)$ in the supercooled liquid has been described by VFT equations (red solid lines). Red dashed line is the horizontal transfer of the VFT fit of the nearest fully amorphous concentration (see Figure 1a,b). (b) Dielectric spectra obtained after the isothermal and isobar crystallization under given conditions. (c) Experimentally determined concentrations dependencies of the T_g of the FL-PVP/VA mixtures at 0.1, 20, and 50 MPa (gray circles, diamonds, and pentagons, respectively). Dark gray hexagons correspond to the concentrations obtained after the recrystallization under isochronal — τ_α = 2.7 μs — conditions.

fitting parameters determined above, the values of τ_α (and $\tau_{\alpha'}$ for the samples after recrystallization) were calculated by means of the following formula

$$\tau_{\alpha/\alpha'} = \tau_{HN}\left[\sin\left(\frac{\pi a}{2+2b}\right)\right]^{1/a}\left[\sin\left(\frac{\pi ab}{2+2b}\right)\right]^{-1/a} \quad (3)$$

Relaxation times obtained from the above described fitting procedure are presented in Figures 2b, 3a, 4a, and 5a. As can be seen, the FL + 10 wt % PVP/VA system begins to recrystallize at relatively low temperatures (under these conditions, the relaxation time of the sample is far from the desired value — see Figures 2b, 3a, 4a and 5a). Therefore, in order to determine the temperature that corresponds to the chosen τ_α, we decided to use the VFT equation. From the extrapolation of the VFT fit up to the selected relaxation time (e.g., τ_α = 0.13 μs), we were able to determine the temperature of the system (see the brown star in Figure 2b). As can be seen under ambient pressure conditions, the FL + 10 wt % PVP/VA sample needs to be heated up to the 347 K in order to have the relaxation time equal to τ_α = 0.13 μs. This procedure was repeated for samples under each chosen pressure condition (i.e., 0.1, 20, and 50 MPa). Once it was done, we were able to perform isothermal crystallization studies under given conditions in order to determine the solubility limit of the drug within the polymer matrix. Figure 2c presents the representative example of performed recrystallization studies. The presented dielectric spectra show crystallization at 0.1 MPa and 347 K, t_0 indicates the first recorded spectrum at set temperature, and it does not correspond to the beginning of the crystallization because of the sample's tendency toward recrystallization. The light gray dotted spectrum is presented only as a visual aid and was not obtained during any measurement. When the recrystallization of the excess amount of the SM (FL) from the supersaturated system ceased, one well-resolved loss peak—α'-process—was still visible (as in previously reported cases[8,16,26,28,29]), see Figure 2c.

Next, in order to exclude the possibility of correlating this additional process to either segmental or secondary relaxation originating from residual amorphous polymer, remaining after the recrystallization of the whole amount of the drug from the mixture, we followed the procedure proposed in ref 16.

In order to obtain relaxation times in a wide temperature range needed to determine the glass-transition temperature related to the α'-process [$T_g = T(\tau_{\alpha'} = 100$ s)], we cooled down the sample — when no further changes in molecular dynamic of the system were observed (no changes for approx. 15 h, see Figure 2c), during/after crystallization — and then measured it again during heating. As can be observed in Figure 2a (brown lines), during this measurement, the dielectric spectra of the examined sample have been registered up to the temperature of the performed isothermal crystallization (e.g., 347 K). Dielectric spectra obtained throughout this procedure, just as the spectra of the fully amorphous sample, were then fitted using the HN fitting function (see Figure 2a).

Determination of the origin of this additional process was possible, once the temperature dependence of the α'-relaxation times [$\tau_{\alpha'}(T)$] of the partially recrystallized sample was obtained. Because of the nonlinear behavior of $\tau_{\alpha'}(T)$ and the fact that it follows the VFT equation (see brown circles in Figure 2b), one can easily conclude that the α'-process is the primary relaxation process of different than initial concen-

https://dx.doi.org/10.1021/acs.molpharmaceut.0c00463
Mol. Pharmaceutics 2020, 17, 3730−3739

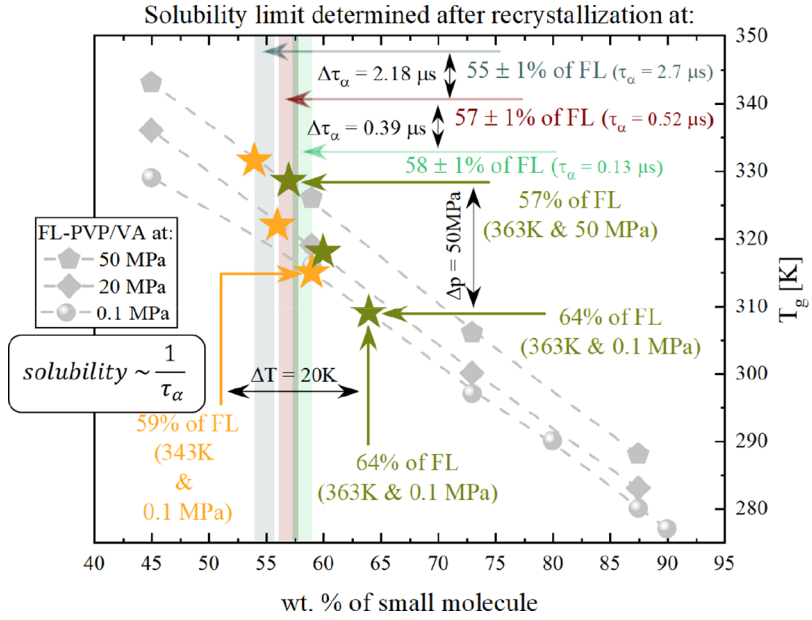

Figure 6. Experimentally determined concentrations dependencies of the T_g of the FL-PVP/VA mixtures at 0.1, 20, and 50 MPa (gray circles, diamonds, and pentagons, respectively). Green and orange stars correspond to the T_g value of the concentrations obtained after isothermal recrystallizations at 363 and 343 K, respectively, at 0.1, 20, and 50 MPa. Wine and light green shadowed area correspond to the concentrations obtained after the recrystallization under isochronal — τ_α = 0.52 μs and 0.13 μs — conditions.

tration of the drug in the FL-PVP/VA system. We determined its T_g value by extrapolation of its VFT fit to 100 s. Thus, the saturated FL-PVP/VA system established under 347 K and 0.1 MPa conditions is characterized by a glass-transition temperature equal to 314 K (see Figure 2b). Next, by following this procedure in the case of the studies performed at elevated pressure, we determined the T_g of the saturated systems. Similarly, as in the case of the measurements, analyzed at the beginning of this work, the number of the experimentally determined τ_α after recrystallization at elevated pressure is not sufficient to parameterize it well with the VFT equation. This can be explained by the increased dc conductivity contribution during BDS measurements at elevated pressure. Therefore, we decided to transfer horizontally the VFT fit of the FL + 41 wt % PVP/VA system to match determined $\tau_\alpha(T)$ (red dashed line in Figure 3a, 4a and 5a).

Figure 3a presents the $\tau_\alpha(T)$s registered for the fully amorphous FL + 10 wt % of PVP/VA (at 0.1, 20, and 50 MPa) samples as well as these samples after crystallization under isochronal conditions (τ_α = 0.13 μs): (i) 363 K and 50 MPa; (ii) 353 K and 20 MPa; (iii) 347 K and 0.1 MPa (blue pentagons, turquoise diamonds, and dark green circles, respectively). Dielectric spectra obtained when the recrystallization process ceased exhibit one extraordinary feature, and despite different temperature and pressure conditions, they all had been characterized by the same relaxation time — determined based on the HN fit — τ_α = 1.27 ms (see Figure 3b). It is interesting that the recrystallization carried out under the conditions that correspond to $\tau_{\alpha\text{-}1}$ ceases at certain — different than initial — $\tau_{\alpha\text{-}2}$. By applying the procedure discussed in this work, we determined the T_gs of the saturated systems. By comparing the obtained values to the previously reported T_g to concentrations dependencies of the FL-PVP/VA mixtures at 0.1,[16] 20, and 50 MPa[26] we were able to identify the concentration of the tested system. As can be seen in Figure 3c, the concentrations obtained by the recrystallization under conditions that correspond with τ_α = 0.13 μs are equal to 57, 58, and 59 wt % at 50, 20, and 0.1 MPa, respectively. It has to be pointed out that small differences between determined concentrations might be due to the, for example, extrapolation of the VFT fits and/or small number of the experimental data after the recrystallization of the sample (because of the increased dc conductivity contribution during BDS measurements at elevated pressure).

To confirm the validity of our assumption that τ_α is the key to maintain the desired solubility limit of a SM within the polymer matrix at elevated pressure, we conduct additional measurements for different initial τ_α. Namely, we performed recrystallization measurements under isochronal conditions (τ_α = 0.52 and 2.7 μs): (i) 353 and 343 K at 50 MPa; (ii) 343 and 334 K at 20 MPa; (iii) 336 and 327 K at 0.1 MPa (Figures 4a and 5a: blue pentagons, turquoise diamonds, and dark green circles, respectively).

Analogously as in previously chosen τ_α when the recrystallization ceased, dielectric spectra collected under various sets of temperature and pressure conditions have been characterized by the exact same relaxation time: τ_α = 13 ms (see Figure 4b) and τ_α = 0.3 s (see Figure 5b). Moreover, as can be seen in Figures 4c and 5c, concentrations obtained by the recrystallization of the excess amount of the drug under isochronal conditions are equal to 56, 57, and 58 wt % at 50, 20, and 0.1 MPa, respectively, while starting at τ_α = 0.52 μs and 54, 55, and 56 wt % at 50, 20, and 0.1 MPa, respectively, while starting at (τ_α = 2.7 μs). Once again small deviations between determined concentrations are present; the explanation of which has already been given. However, one can observe that there is a constant difference between the solubility limit obtained while starting from τ_α = 2.7 μs, 0.52 μs or 0.13 μs. It has to be pointed out that in all presented cases of chosen τ_α (as a starting point for the recrystallization) systems reach a defined solubility, based on their initial relaxation time.

Comparing the solubility limit values obtained during the recrystallization at constant pressure, constant temperature, and constant relaxation time, one can notice some significant

https://dx.doi.org/10.1021/acs.molpharmaceut.0c00463
Mol. Pharmaceutics 2020, 17, 3730−3739

differences (see Figure 6). Namely, maintaining the constant pressure (either for 0.1 MPa or 50 MPa), while altering the temperature, we obtained the generally accepted dependence between temperature and solubility limits — the higher the temperature, the larger amount of the SMs (in our case FL) can be successfully dissolved within the polymer matrix[5,10,11,15,17−24] (e.g., 59 wt % of FL at 343 K and 64 wt % of FL at 363 K for 0.1 MPa). On the other hand, recrystallization conducted at a constant temperature (either 343 or 363 K—orange and green stars, respectively, in Figure 6), while applying different pressures, results in the following: with increasing pressure, the solubility of the FL within the polymer matrix is decreasing (e.g., 64 wt % of FL at 0.1 MPa and 57 wt % of FL at 50 MPa for 363 K) — effect similar to decreasing temperature at constant pressure. However, measurements carried out at the same relaxation time (either for τ_α = 2.7 μs or τ_α = 0.13 μs), regardless of chosen set of temperature and pressure conditions, results in the same concentration—the same solubility limit (e.g., approx. 55 wt % of FL for τ_α = 2.7 μs and 58 wt % of FL for τ_α = 0.13 μs), which confirms the initial assumption that the solubility of the SMs (e.g., FL) within the polymer matrix is inversely proportional to the τ_α of their system ($S \sim 1/\tau_\alpha$).

It should be pointed out that our understanding of the role of the isochronal conditions in the solubility limit studies is still limited and thus the role of many factors (e.g., drug−polymer interactions) is yet to be understood. The mentioned interactions have been known to affect both the thermodynamics and kinetics of the precipitation.[47−49] Although in recent study Prasad et al. showed (on the example of indomethacin drug) that despite the fact that both used polymers (Eudragit E100 and PVP K90) interfere with the kinetics of precipitation via drug−polymer interactions no significant change in solubility was observed with any of the added polymers,[50] one has to acknowledge that drug−polymer interactions might either inhibit or induce precipitation (crystal growth or nucleation) in a manner that is difficult to predict, which in turn could affect the extent and duration of supersaturation.[51,52] Furthermore, the complexity of this issue increases when one considers the additional factor — elevated pressure. The densification of the molecular packing of the system is a direct result of the applied high pressure and can lead to the improvement of drug−polymer interactions[53] or vice versa the weakening of hydrogen bonding between drug and polymer.[54]

Nevertheless, we strongly believe that this approach along with the dielectric measurement might become an irreplaceable tool in predicting the limiting polymer concentration for the extrusion-based manufacturing purposes. Even though one might conclude, based on the presented results, that there is a potential risk, that a change in the solubility limit caused by the elevated pressure might lead to recrystallization of the excess amount of the drug during the extrusion process, the presented idea has not yet been tested during production conditions. Therefore, we strongly encourage further exploration of this kind of behavior.

CONCLUSIONS

To summarize, the presented experimental results confirm that regardless of the chosen temperature or pressure, while sustaining the same initial relaxation time, one would maintain a desired level of solubility. Furthermore, it seems that the elevated pressure compensates the effect of solubility enhancement caused by the elevated temperature. Such information is not only of fundamental relevance in science but also, from a much broader perspective, could be potentially very useful considering extrusion-based manufacturing methods. However, it is but a first step toward the validation of the proposed idea: mutual dependence between the solubility of all SMs within the polymers and τ_α of their systems.

AUTHOR INFORMATION

Corresponding Author

Krzysztof Chmiel − *Faculty of Science and Technology, Institute of Physics, University of Silesia, SMCEBI, 41-500 Chorzów, Poland;* orcid.org/0000-0003-4532-0051; Email: krzysztof.chmiel@smcebi.edu.pl

Authors

Justyna Knapik-Kowalczuk − *Faculty of Science and Technology, Institute of Physics, University of Silesia, SMCEBI, 41-500 Chorzów, Poland;* orcid.org/0000-0003-3736-8098

Marian Paluch − *Faculty of Science and Technology, Institute of Physics, University of Silesia, SMCEBI, 41-500 Chorzów, Poland*

Complete contact information is available at: https://pubs.acs.org/10.1021/acs.molpharmaceut.0c00463

Notes

The authors declare no competing financial interest.

ACKNOWLEDGMENTS

The authors, K.C., J.K.-K., and M.P., are grateful for the financial support received within the project no. 2015/16/W/NZ7/00404 (SYMFONIA 3) from the National Science Centre, Poland.

REFERENCES

(1) Flory, P. J. Thermodynamics of High Polymer Solutions. *J. Chem. Phys.* **1942**, *10*, 51−61.

(2) Flory, P. J.. Principles of polymer chemistry; Cornell University Press, 1953, https://books.google.pl/books/about/Principles_of_Polymer_Chemistry.html?id=CQ0EbEkT5R0C&redir_esc=y (accessed March 4, 2019).

(3) Nishi, T.; Wang, T. T. Melting Point Depression and Kinetic Effects of Cooling on Crystallization in Poly(vinylidene fluoride)-Poly(methyl methacrylate) Mixtures. *Macromolecules* **1975**, *8*, 909−915.

(4) Hansen, C. M. The three-dimensional solubility parameter - key to paint component affinities: solvents, plasticizers, polymers, and resins. II. Dyes, emulsifiers, mutual solubility and compatibility, and pigments. III. Independent cal-culation of the parameter components. *J. Paint Technol.* **1967**, *39*, 505−510. . http://www.bcin.ca/bcin/detail.app?id=51777 (accessed January 8, 2019)

(5) Tao, J.; Sun, Y.; Zhang, G. G. Z.; Yu, L. Solubility of small-molecule crystals in polymers: D-Mannitol in PVP, indomethacin in PVP/VA, and nifedipine in PVP/VA. *Pharm. Res.* **2009**, *26*, 855−864.

(6) Höhne, G. W. H.; Hemminger, W. F.; Flammersheim, H.-J. *Differential Scanning Calorimetry*; Springer Berlin Heidelberg: Berlin, Heidelberg, 2003.

(7) Tian, Y.; Booth, J.; Meehan, E.; Jones, D. S.; Li, S.; Andrews, G. P. Construction of drug-polymer thermodynamic phase diagrams using flory-huggins interaction theory: Identifying the relevance of temperature and drug weight fraction to phase separation within solid dispersions. *Mol. Pharm.* **2013**, *10*, 236−248.

(8) Knapik-Kowalczuk, J.; Chmiel, K.; Jurkiewicz, K.; Wojnarowska, Z.; Kurek, M.; Jachowicz, R.; Paluch, M. Influence of Polymeric

Additive on the Physical Stability and Viscoelastic Properties of Aripiprazole. *Mol. Pharm.* **2019**, *16*, 1742−1750.
(9) Lehmkemper, K.; Kyerematen, S. O.; Bartels, M.; Degenhardt, M.; Sadowski, G. Physical stability of API/polymer-blend amorphous solid dispersions. *Eur. J. Pharm. Biopharm.* **2018**, *124*, 147−157.
(10) Tamagawa, R. E.; Martins, W.; Derenzo, S.; Bernardo, A.; Rolemberg, M. P.; Carvan, P.; Giulietti, M. Short-Cut Method To Predict the Solubility of Organic Molecules in Aqueous and Nonaqueous Solutions by Differential Scanning Calorimetry. *Cryst. Growth Des.* **2006**, *6*, 313−320.
(11) Mahieu, A.; Willart, J.-F.; Dudognon, E.; Danède, F.; Descamps, M. A New Protocol To Determine the Solubility of Drugs into Polymer Matrixes. *Mol. Pharm.* **2013**, *10*, 560−566.
(12) Marsac, P. J.; Li, T.; Taylor, L. S. Estimation of drug-polymer miscibility and solubility in amorphous solid dispersions using experimentally determined interaction parameters. *Pharm. Res.* **2009**, *26*, 139−151.
(13) Gross, J.; Sadowski, G. Perturbed-chain SAFT: An equation of state based on a perturbation theory for chain molecules. *Ind. Eng. Chem. Res.* **2001**, *40*, 1244−1260.
(14) Gross, J.; Sadowski, G. Modeling polymer systems using the perturbed-chain statistical associating fluid theory equation of state. *Ind. Eng. Chem. Res.* **2002**, *41*, 1084−1093.
(15) Sun, Y.; Tao, J.; Zhang, G. G. Z.; Yu, L. Solubilities of Crystalline Drugs in Polymers: An Improved Analytical Method and Comparison of Solubilities of Indomethacin and Nifedipine in PVP, PVP/VA, and PVAc. *J. Pharm. Sci.* **2010**, *99*, 4023−4031.
(16) Chmiel, K.; Knapik-Kowalczuk, J.; Jurkiewicz, K.; Sawicki, W.; Jachowicz, R.; Paluch, M. A New Method To Identify Physically Stable Concentration of Amorphous Solid Dispersions (1): Case of Flutamide + Kollidon VA64. *Mol. Pharm.* **2017**, *14*, 3370−3380.
(17) Mohan, R.; Lorenz, H.; Myerson, A. S. Solubility measurement using differential scanning calorimetry. *Ind. Eng. Chem. Res.* **2002**, *41*, 4854−4862.
(18) Park, K.; Evans, J. M. B.; Myerson, A. S. Determination of Solubility of Polymorphs Using Differential Scanning Calorimetry. *Cryst. Growth Des.* **2003**, *3*, 991−995.
(19) Qian, F.; Huang, J.; Hussain, M. A. Drug−Polymer Solubility and Miscibility: Stability Consideration and Practical Challenges in Amorphous Solid Dispersion Development. *J. Pharm. Sci.* **2010**, *99*, 2941−2947.
(20) Zhao, Y.; Inbar, P.; Chokshi, H. P.; Malick, A. W.; Choi, D. S. Prediction of the thermal phase diagram of amorphous solid dispersions by flory-huggins theory. *J. Pharm. Sci.* **2011**, *100*, 3196−3207.
(21) Kozyra, A.; Mugheirbi, N. A.; Paluch, K. J.; Garbacz, G.; Tajber, L., Phase Diagrams of Polymer-Dispersed Liquid Crystal Systems of Itraconazole/Component Immiscibility Induced by Molecular Anisotropy, (**2018**, *15*). 5192 doi: DOI: 10.1021/acs.molpharmaceut.8b00724.
(22) Potter, C. B.; Davis, M. T.; Albadarin, A. B.; Walker, G. M. Investigation of the Dependence of the Flory−Huggins Interaction Parameter on Temperature and Composition in a Drug−Polymer System. *Mol. Pharm.* **2018**, *15*, 5327−5335.
(23) Greenhalgh, D. J.; Williams, A. C.; Timmins, P.; York, P. Solubility parameters as predictors of miscibility in solid dispersions. *J. Pharm. Sci.* **1999**, *88*, 1182−1190.
(24) Tihic, A.; Kontogeorgis, G. M.; von Solms, N.; Michelsen, M. L.; Constantinou, L. A Predictive Group-Contribution Simplified PC-SAFT Equation of State: Application to Polymer Systems. *Ind. Eng. Chem. Res.* **2008**, *47*, 5092−5101.
(25) Chakravarty, P.; Lubach, J. W.; Hau, J.; Nagapudi, K. A rational approach towards development of amorphous solid dispersions: Experimental and computational techniques. *Int. J. Pharm.* **2017**, *519*, 44−57.
(26) Chmiel, K.; Knapik-Kowalczuk, J.; Paluch, M. How does the high pressure affects the solubility of the drug within the polymer matrix in solid dispersion systems. *Eur. J. Pharm. Biopharm.* **2019**, *143*, 8−17.
(27) Goff, J.; Whelan, T. *The DYNISCO Extrusion Processors Handbook*, 2nd ed.; DYNISCO, 2000.
(28) Chmiel, K.; Knapik-Kowalczuk, J.; Jachowicz, R.; Paluch, M. Broadband dielectric spectroscopy as an experimental alternative to calorimetric determination of the solubility of drugs into polymer matrix: Case of flutamide and various polymeric matrixes. *Eur. J. Pharm. Biopharm.* **2019**, *136*, 231−239.
(29) Pacult, J.; Rams-Baron, M.; Chmiel, K.; Jurkiewicz, K.; Antosik, A.; Szafraniec, J.; Kurek, M.; Jachowicz, R.; Paluch, M. How can we improve the physical stability of co-amorphous system containing flutamide and bicalutamide? The case of ternary amorphous solid dispersions. *Eur. J. Pharm. Sci.* **2019**, *136*, 104947.
(30) Grzybowska, K.; Chmiel, K.; Knapik-Kowalczuk, J.; Grzybowski, A.; Jurkiewicz, K.; Paluch, M. Molecular Factors Governing the Liquid and Glassy States Recrystallization of Celecoxib in Binary Mixtures with Excipients of Different Molecular Weights. *Mol. Pharm.* **2017**, *14*, 1154−1168.
(31) Atawa, B.; Correia, N. T.; Couvrat, N.; Affouard, F.; Coquerel, G.; Dargent, E.; Saiter, A. Molecular mobility of amorphous N-acetyl-α-methylbenzylamine and Debye relaxation evidenced by dielectric relaxation spectroscopy and molecular dynamics simulations. *Phys. Chem. Chem. Phys.* **2019**, *21*, 702−717.
(32) Szymoniak, P.; Madkour, S.; Schönhals, A. Molecular Dynamics of the Asymmetric Blend PVME/PS Revisited by Broadband Dielectric and Specific Heat Spectroscopy: Evidence of Multiple Glassy Dynamics. *Macromolecules* **2019**, *52*, 1620−1631.
(33) Roland, C. M.; Hensel-Bielowka, S.; Paluch, M.; Casalini, R. Supercooled dynamics of glass-forming liquids and polymers under hydrostatic pressure. *Rep. Prog. Phys.* **2005**, *68*, 1405−1478.
(34) Adrjanowicz, K.; Winkler, R.; Dzienia, A.; Paluch, M.; Napolitano, S., Connecting 1D and 2D Confined Polymer Dynamics to Its Bulk Behavior via Density Scaling, (**2019**, *8*). 304 doi: DOI: 10.1021/acsmacrolett.8b01006.
(35) Adrjanowicz, K.; Kaminski, K.; Wojnarowska, Z.; Dulski, M.; Hawelek, L.; Pawlus, S.; Paluch, M.; Sawicki, W. Dielectric Relaxation and Crystallization Kinetics of Ibuprofen at Ambient and Elevated Pressure. *J. Phys. Chem. B* **2010**, *114*, 6579−6593.
(36) Knapik-Kowalczuk, J.; Wojnarowska, Z.; Rams-Baron, M.; Jurkiewicz, K.; Cielecka-Piontek, J.; Ngai, K. L.; Paluch, M. Atorvastatin as a Promising Crystallization Inhibitor of Amorphous Probucol: Dielectric Studies at Ambient and Elevated Pressure. *Mol. Pharm.* **2017**, *14*, 2670−2680.
(37) Knapik, J.; Wojnarowska, Z.; Grzybowska, K.; Tajber, L.; Mesallati, H.; Paluch, K. J.; Paluch, M. Molecular Dynamics and Physical Stability of Amorphous Nimesulide Drug and Its Binary Drug-Polymer Systems. *Mol. Pharm.* **2016**, *13*, 1937−1946.
(38) Wojnarowska, Z.; Adrjanowicz, K.; Wlodarczyk, P.; Kaminska, E.; Kaminski, K.; Grzybowska, K.; Wrzalik, R.; Paluch, M.; Ngai, K. L. Broadband Dielectric Relaxation Study at Ambient and Elevated Pressure of Molecular Dynamics of Pharmaceutical: Indomethacin. *J. Phys. Chem. B* **2009**, *113*, 12536−12545.
(39) Vogel, H. Temperaturabhangigkeitgesetz der Viskosität von Flüssigkeiten. *J. Phys. Z.* **1921**, 645−646. . https://scholar.google.pl/scholar?hl=pl&as_sdt=0%2C5&q=Vogel+H.%3B+J.+Phys.+Z.+1921%2C+22%2C+645-646&btnG=&oq=J+phys+Z (accessed October 3, 2017)
(40) Fulcher, G. S. ANALYSIS OF RECENT MEASUREMENTS OF THE VISCOSITY OF GLASSES. *J. Am. Ceram. Soc.* **1925**, *8*, 339−355.
(41) Tammann, G.; Hesse, W. Die Abhängigkeit der Viscosität von der Temperatur bie unterkühlten Flüssigkeiten. *Z. Anorg. Allg. Chem.* **1926**, *156*, 245−257.
(42) Marsac, P. J.; Shamblin, S. L.; Taylor, L. S. Theoretical and practical approaches for prediction of drug-polymer miscibility and solubility. *Pharm. Res.* **2006**, *23*, 2417−2426.
(43) Rask, M. B.; Knopp, M. M.; Olesen, N. E.; Holm, R.; Rades, T. Influence of PVP/VA copolymer composition on drug−polymer solubility. *Eur. J. Pharm. Sci.* **2016**, *85*, 10−17.

https://dx.doi.org/10.1021/acs.molpharmaceut.0c00463
Mol. Pharmaceutics 2020, 17, 3730−3739

(44) Rams-Baron, M.; Wojnarowska, Z.; Grzybowska, K.; Dulski, M.; Knapik, J.; Jurkiewicz, K.; Smolka, W.; Sawicki, W.; Ratuszna, A.; Paluch, M. Toward a Better Understanding of the Physical Stability of Amorphous Anti-Inflammatory Agents: The Roles of Molecular Mobility and Molecular Interaction Patterns. *Mol. Pharm.* **2015**, *12*, 3628−3638.
(45) Knapik, J.; Wojnarowska, Z.; Grzybowska, K.; Jurkiewicz, K.; Stankiewicz, A.; Paluch, M. Stabilization of the Amorphous Ezetimibe Drug by Confining Its Dimension. *Mol. Pharm.* **2016**, *13*, 1308−1316.
(46) Kremer, F.; Schönhals, A. *Broadband Dielectric Spectroscopy*; Springer, 2003.
(47) Ojarinta, R.; Saarinen, J.; Strachan, C. J.; Korhonen, O.; Laitinen, R. Preparation and characterization of multi-component tablets containing co-amorphous salts: Combining multimodal non-linear optical imaging with established analytical methods. *Eur. J. Pharm. Biopharm.* **2018**, *132*, 112−126.
(48) Wong, J. J. L.; Yu, H.; Lim, L. M.; Hadinoto, K. A trade-off between solubility enhancement and physical stability upon simultaneous amorphization and nanonization of curcumin in comparison to amorphization alone. *Eur. J. Pharm. Sci.* **2018**, *114*, 356−363.
(49) Lu, J.; Obara, S.; Liu, F.; Fu, W.; Zhang, W.; Kikuchi, S. Melt Extrusion for a High Melting Point Compound with Improved Solubility and Sustained Release. *AAPS PharmSciTech* **2018**, *19*, 358−370.
(50) Prasad, D.; Chauhan, H.; Atef, E., Role of Molecular Interactions for Synergistic Precipitation Inhibition of Poorly Soluble Drug in Supersaturated Drug−Polymer−Polymer Ternary Solution, (**2016**, *13*). 756 doi: DOI: 10.1021/acs.molpharmaceut.5b00655.
(51) Alonzo, D. E.; Raina, S.; Zhou, D.; Gao, Y.; Zhang, G. G. Z.; Taylor, L. S. Characterizing the impact of hydroxypropylmethyl cellulose on the growth and nucleation kinetics of felodipine from supersaturated solutions. *Cryst. Growth Des.* **2012**, *12*, 1538−1547.
(52) Ilevbare, G. A.; Liu, H.; Edgar, K. J.; Taylor, L. S. Understanding polymer properties important for crystal growth inhibition-impact of chemically diverse polymers on solution crystal growth of ritonavir. *Cryst. Growth Des.* **2012**, *12*, 3133−3143.
(53) Worku, Z. A.; Aarts, J.; Van den Mooter, G. Influence of Compression Forces on the Structural Stability of Naproxen/PVP-VA 64 Solid Dispersions. *Mol. Pharm.* **2014**, *11*, 1102−1108.
(54) Ayenew, Z.; Paudel, A.; Van den Mooter, G. Can compression induce demixing in amorphous solid dispersions? A case study of naproxen−PVP K25. *Eur. J. Pharm. Biopharm.* **2012**, *81*, 207−213.

https://dx.doi.org/10.1021/acs.molpharmaceut.0c00463
Mol. Pharmaceutics 2020, 17, 3730−3739